Structures of glycosylated mammalian glutaminyl cyclases reveal conformational variability near the active center

Supporting Information

David Ruiz Carrillo[1,2§], Birgit Koch[1§], Christoph Parthier[2], Michael Wermann[1], Tresfore Dambe[3], Mirko Buchholz[1], Hans-Henning Ludwig[1], Ulrich Heiser[1], Jens-Ulrich Rahfeld[1], Milton T. Stubbs[2,4*], Stephan Schilling[1*], and Hans-Ulrich Demuth[1].

Addresses: [1]Probiodrug AG, Weinbergweg 22, D-06120 Halle (Saale), [2]Institut für Biochemie und Biotechnologie, Martin-Luther-Universität Halle-Wittenberg, Kurt-Mothes-Straße 3, D-06120 Halle (Saale), [3]PSF AG, Robert-Roessle-Straße 10, D-13092 Berlin, Germany, [4]Mitteldeutsches Zentrum für Struktur und Dynamik der Proteine (MZP), Martin-Luther-Universität Halle-Wittenberg, D-06099 Halle (Saale), Germany

Running head: Structures of murine and human glutaminyl cyclases

§ these authors contributed equally to this work

***To whom correspondence may be addressed:**

Stephan Schilling, Probiodrug AG, Weinbergweg 22, D-06120 Halle (S), Germany, tel.: +49 345 5559900, fax: +49 345 5559901;
E-mail: Stephan.Schilling@probiodrug.de

Milton T. Stubbs, Institut für Biochemie und Biotechnologie, Martin-Luther-Universität Halle-Wittenberg, Kurt-Mothes-Straße 3, D-06120 Halle (S), Germany, tel: +49 345 55 24901, fax: +49 345 55 27360;
E-mail: stubbs@biochemtech.uni-halle.de

Table S1: Comparison of the kinetic parameters of human QC recombinantly expressed by different systems

substrate	k_{cat}/K_m [$mM^{-1}s^{-1}$]	expression system	reference
Gln-NH_2	8.7	*P. pastoris*	[1]this study
	0.1	*E. coli*	[2]Song *et al*
	0.4	*E. coli*	[3]Bateman *et al.*
	9.3	*Drosophila* S2 cells	[4]Booth *et al.*
Gln-Gln-OH	84.2	*P. pastoris*	this study
	1.3	*E. coli*	Song *et al.*
	13.7	*E. coli*	[5a]Huang *et al.*
	14.3	*Drosophila* S2 cells	Booth *et al.*
Gln-tert-butyl ester	5.6	*P. pastoris*	[6]Schilling *et al.*
	5.1	*E. coli*	Huang *et al.*
	2.4	*Drosophila* S2 cells	Booth *et al.*
Gln-Gly-OH	19.9	*P. pastoris*	this study
	0.2	*E. coli*	Song *et al.*
Gln-Ala-OH	249	*P. pastoris*	Schilling *et al.*
	1	*E. coli*	Song *et al.*
Gln-βNA	144	*P. pastoris*	this study
	93	*E. coli*	[5b]Huang *et al.*

[1]reaction conditions: 50mM Tris, pH8; 30°C

[2]Song, I., Chuang, C. Z., and Bateman, R. C. J. (1994) *J Mol Endocrinol 13*, 77-86.
reaction conditions: 50mM *N*-Tris(hydroxymethyl)methyl-2-aminoethanesulfonic acid (Tes), pH7.8; 400mM NaCl; 37°C

[3]Bateman, R. C., Temple, J. S., Misquitta, S. A., and Booth, R. E. (2001) *Biochemistry 40*, 11246-11250.
reaction conditions: 50mM *N*-Tris(hydroxymethyl)methyl-2-aminoethanesulfonic acid (Tes), pH7.8; 400mM NaCl; 37°C

[4]Booth, R. E., Misquitta, S. A., and Bateman, R. C., Jr. (2003) *Protein Expr. Purif. 32*, 141-146.
reaction conditions: 50mM Tris, pH8; 37°C

[5a]Huang, K.F., Liu, Y.L., Wang, A.H. (2005) *Protein Expr. Purif. 43*, 65-72.

[5b]Huang, K.F., Wang, Y.R., Chang, E.C., Chou, T.L.; Wang, A.H. (2008) *Biochem. J. 411*, 181-190
reaction conditions: 50mM Tris, pH8; 25°C

[6]Schilling, S., Manhart, S., Hoffmann, T., Ludwig, H.-H., Wasternack, C., and Demuth, H.-U. (2003) *Biol Chem 384*, 1583-1592.
reaction conditions: 50mM Tris, pH8; 30°C

Table S2: Oligonucleotides applied for cloning and mutation of hQC WT and variants

primer	sequence (5' – 3')	purpose
$C_{s\ (sense)}$	ATATATCTGCA|GCG CAT CAC CAT CAC CAT CAC |→hQC GAG GAG AAG AAT TAC CAC C (*Pst*1)	cloning
$C_{as\ (antisense)}$	ATATATGC|GGCCGC TTA CAA ATG AAG ATA TTC C (*Not*1, |→hQC)	cloning
S_s	GGA GCC ACT GAT TCA GCC G	sequencing
S_{as}	CTG GAG TGA CAA ATC TGG C	sequencing
$C^{139}A_s$	CAT TTG GTC CTC GCC **GCC** CAC TAT GAC TCC AAG	$C^{139}A$
$C^{139}A_{as}$	CTT GGA GTC ATA GTG **GGC** GGC GAG GAC CAA ATG	$C^{139}A$
$C^{164}A_s$	GAT TCA GCC GTG CCA **GCT** GCA ATG ATG TTG GAA C	$C^{164}A$
$C^{164}A_{as}$	G TTC CAA CAT CAT TGC **AGC** TGG CAC GGC TGA ATC	$C^{164}A$
$W^{207}A_s$	GAG GCT TTT CTT CAC **GCG** TCT CCT CAA GAT TC	$W^{207}A$
$W^{207}A_{as}$	GA ATC TTG AGG AGA **CGC** GTG AAG AAA AGC CTC	$W^{207}A$
$W^{207}F_s$	GAG GCT TTT CTT CAC **TTT** TCT CCT CAA GAT TC	$W^{207}F$
$W^{207}F_{as}$	GA ATC TTG AGG AGA **AAA** GTG AAG AAA AGC CTC	$W^{207}F$
$W^{207}L_s$	GAG GCT TTT CTT CAC **CTG** TCT CCT CAA GAT TC	$W^{207}L$
$W^{207}L_{as}$	GA ATC TTG AGG AGA **CAG** GTG AAG AAA AGC CTC	$W^{207}L$
$W^{207}Q_s$	GAG GCT TTT CTT CAC **CAG** TCT CCT CAA GAT TC	$W^{207}Q$
$W^{207}Q_{as}$	GA ATC TTG AGG AGA **CTG** GTG AAG AAA AGC CTC	$W^{207}Q$

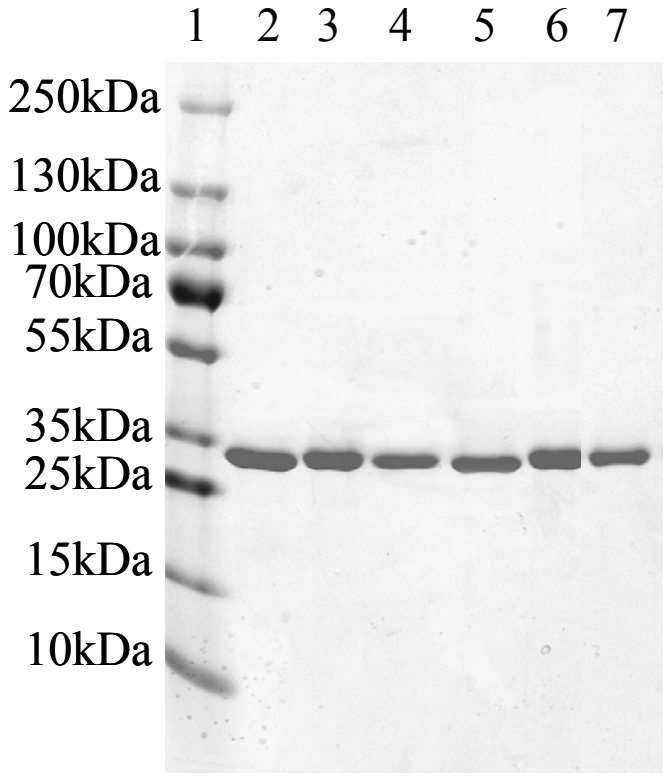

Figure S1: Characterization of hQC WT and mutants by SDS-PAGE. Lanes: 1, molecular mass standards (PageRuler Plus Prestained Protein Ladder, Fermentas, St. Leon-Rot, Germany); 2, $W^{207}A$; 3, $W^{207}F$; 4, $W^{207}L$; 5, $W^{207}Q$; 6, hQC WT; 7, $C^{139}A/C^{164}A$. SDS-Page was performed in 4-20% Tris-Glycine gradient gels (Servagel TG 4-20, Serva, Heidelberg, Germany). Proteins were deglycosylated by endoglycosidase H_f treatment and visualized by Coomassie Blue staining.

Table S3: Summary of data set statistics for crystals of human and mouse QC and their corresponding data processing and model building.

Data collection	hQC & imidazole	mQC-free	mQC-PQ50
Data set collected at	Bessy-MX BL14.1	Bessy-MX BL14.1	Bessy-MX BL14.1
Space group	C2	$P2_12_12_1$	$P2_12_12_1$
Cell dimensions			
a, *b*, *c* (Å)	82.4 63.7 77.2	43.2 86.9 97.2	42.7 83.0 95.7
α, β, γ (°)	90.0 105.8 90.0	90.0 90.0 90.0	90.0 90.0 90.0
Resolution (Å)	12.00-2.10	64.82-2.90	19.81-1.80
(highest resolution shell (Å))	(2.21-2.10)	(3.0-2.90)	(1.90-1.80)
R_{merge}	8.1 (40.1)	11.1 (50.8)	10.7 (52.1)
I/σ(I)	7.1 (2.0)	10.1 (2.4)	13.3 (2.3)
Completeness (%)	96.0	100.0	99.8 (99.9)
Redundancy	3.0	4.8	5.7
Refinement			
Resolution (Å)	11.98 – 2.10	20.0-2.9	19.81-1.80
No. reflections (work/test)	20342/1073	8101/426	29995/1579
R_{work} / R_{free}	20.6 /26.3	24.5/30.0	18.4/26.0
No. atoms			
Protein	2535	2629	2622
Sugars	28	30	42
Water	150	52	342
ions	2	1	10
ligands	5	-	22
B-factors (Å^2)-Mean value	36.1	48.3	21.00
Protein	37.2	48.6	19.4
Sugars	67.9	61.9	66.0
Water	12.5	30.0	30.7
ions	24.4	39.1	35.4
ligands	16.8	-	20.7
R.m.s deviations			
Bond lengths (Å)	0.023	0.019	0.015
Bond angles (°)	1.98	2.16	1.637
Ramachandran analysis(%)			
Favoured	88.6	56.1	88.4
Allowed	11.4	37.2	11.6
Generously allowed	0	6.3	0
Disallowed	0	0.4	0
PDB code	3SI0	3SI1	3SI2

The programs used for data processing were MOSFLM and SCALA, for molecular replacement PHASER, for refinement REFMAC5 and for model building Coot. All programs belong to the CCP4 suite. Numbers between brackets belong to the outer shell resolution limit.

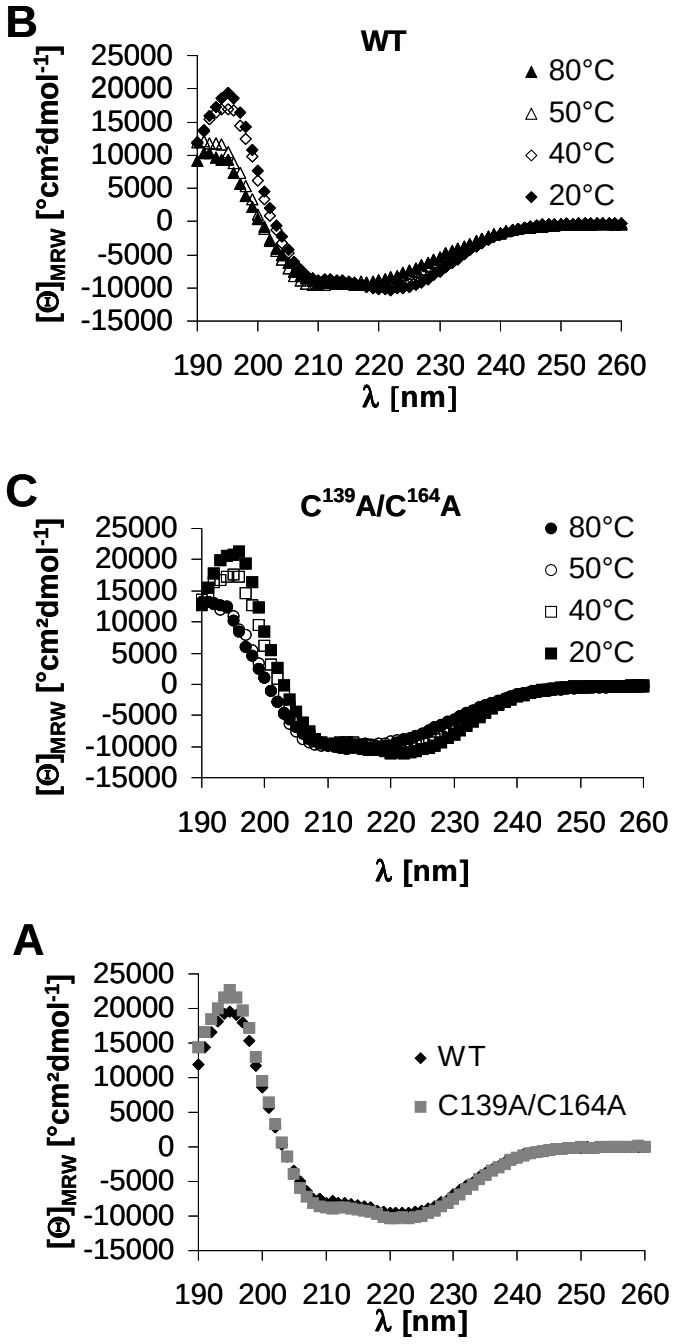

Figure S2: Far UV CD-spectra (190 nm < λ < 260 nm) of hQC WT and hQC variant $C^{139}A/C^{164}A$ lacking the disulfide bond. (A) Comparison of the CD-spectra at 20°C. Both enzymes show a typical CD-spectrum for proteins with a high α-helical content, characterized by minima of the mean residue ellipticity (θ_{MRW}) at 208 nm and 222 nm. (B) CD-spectra of hQC WT at increasing temperature. Unfolding occurs between 40°C and 50°C, indicated by a loss of the θ_{MRW} minimum at 222 nm. (C) CD-spectra of hQC $C^{139}A/C^{164}A$ at increasing temperature. Unfolding occurs between 40°C and 50°C. In contrast to hQC WT, where the spectra at 20°C and 40°C have similar forms, unfolded protein already influences the variant spectrum at 40°C, witnessed by an increased θ_{MRW} around 222 nm. Proteins were dissolved in 10 mM potassium phosphate buffer, pH 6.8.

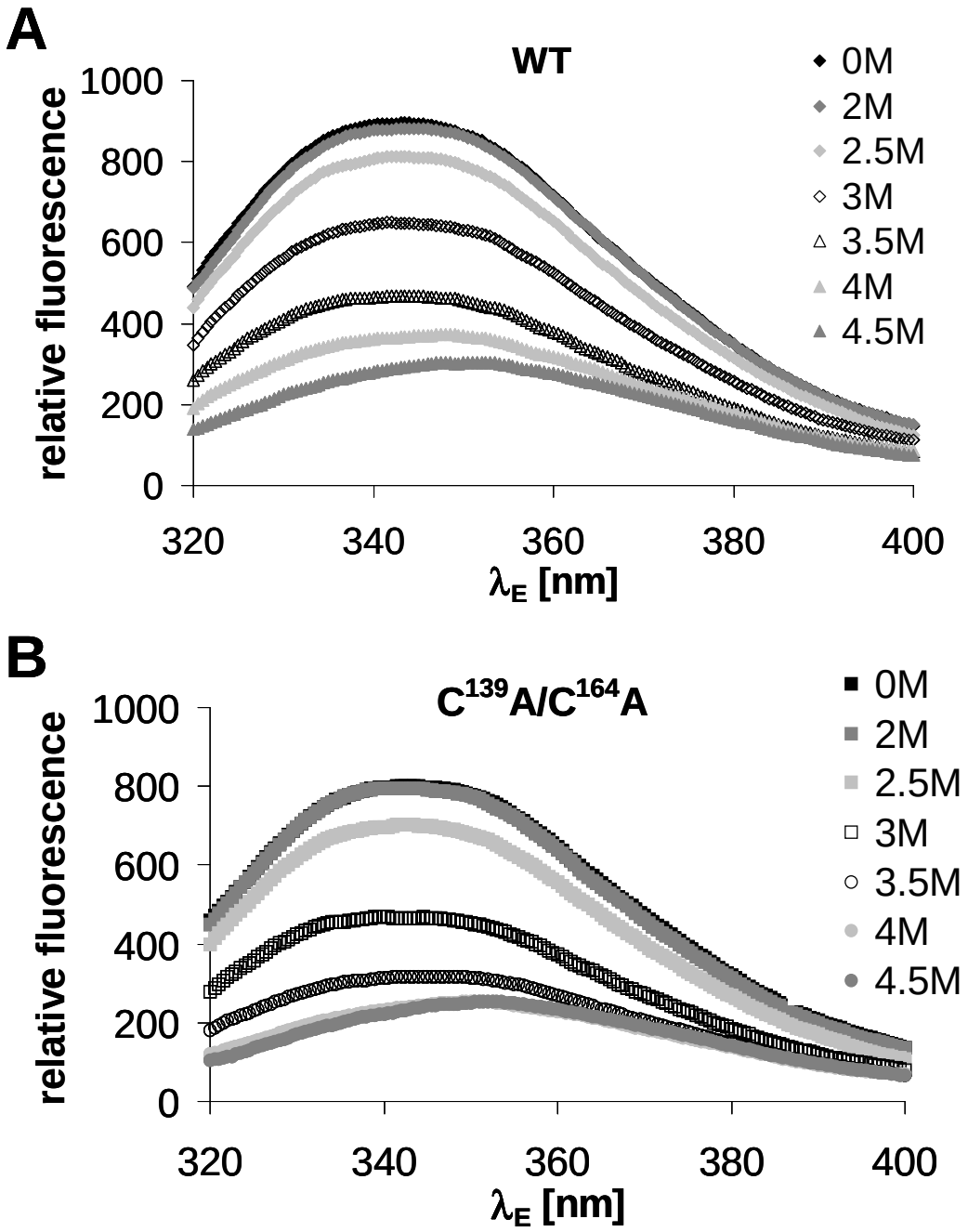

Figure S3: Fluorescence emission spectra (320 nm < $\lambda_{emission}$ < 400 nm) of (A) hQC WT and (B) hQC variant $C^{139}A/C^{164}A$ lacking the disulfide bond at increasing concentrations of GdmCl. Unfolding is characterized by a shift of emission maximum from 354 nm to 344 nm, corresponding to tryptophan emission in a more hydrophilic environment, and a general reduction of the fluorescence emission. Both enzymes are stable until c_{GdmCl} = 2 M; unfolding starts at a GdmCl concentration of 2.5 M. Increasing concentration of GdmCl leads to stronger reduction of the fluorescence emission of the mutant compared to the WT hQC. While there is still a folded fraction of hQC WT at 4 M GdmCl, the $C^{139}A/C^{164}A$ variant is completely unfolded, emphasizing the stabilizing role of the disulfide bond. Proteins were dissolved in 50 mM sodium phosphate buffer, pH 6.8. Data collection was carried out at 22°C and an excitation wavelength of 295 nm.

Table S4: Kinetic constants for hQC WT substrates

Substrate	k_{cat}/K_m [mM s^{-1}]	K_m [μM]	k_{cat} [s^{-1}]
Gln-βNA	144.0 ±0.3	124.0 ± 2.9	17.9 ±0.5
Gln-Gln-OH	84.2 ±0.8	197.6 ± 1.7	8.4 ±0.57
Gln-Glu-OH	35.8 ±2.5	514.8 ±48.4	18.4 ±0.5
Gln-Gly-Pro-OH	84.6 ±3.5	186.1 ±12.3	15.8 ±0.4
Gln-Phe-Ala-NH_2	359.2 ±8.9	118.9 ± 6.6	42.7 ±3.4
Gln-Glu-Asp-Leu-NH_2	250.4 ±9.0	72.1 ± 3.2	18.1 ±0.28
BigGastrin	379.9 ±0.8	53.0 ± 1.3	20.1 ±0.5
Gastrin	16.2 ±8.2	14.2 ± 2.0	1.6 ±0.1
GnRH	290.4 ±2.7	70.9 ± 1.1	20.6 ±0.5
Neurotensin	237.7 ±5.4	68.7 ± 2.2	16.3 ±1.6

K_m and k_{cat} values were determined in three independent evaluations. Reactions were carried out in 50mM Tris, pH 8.0, at 30°C.

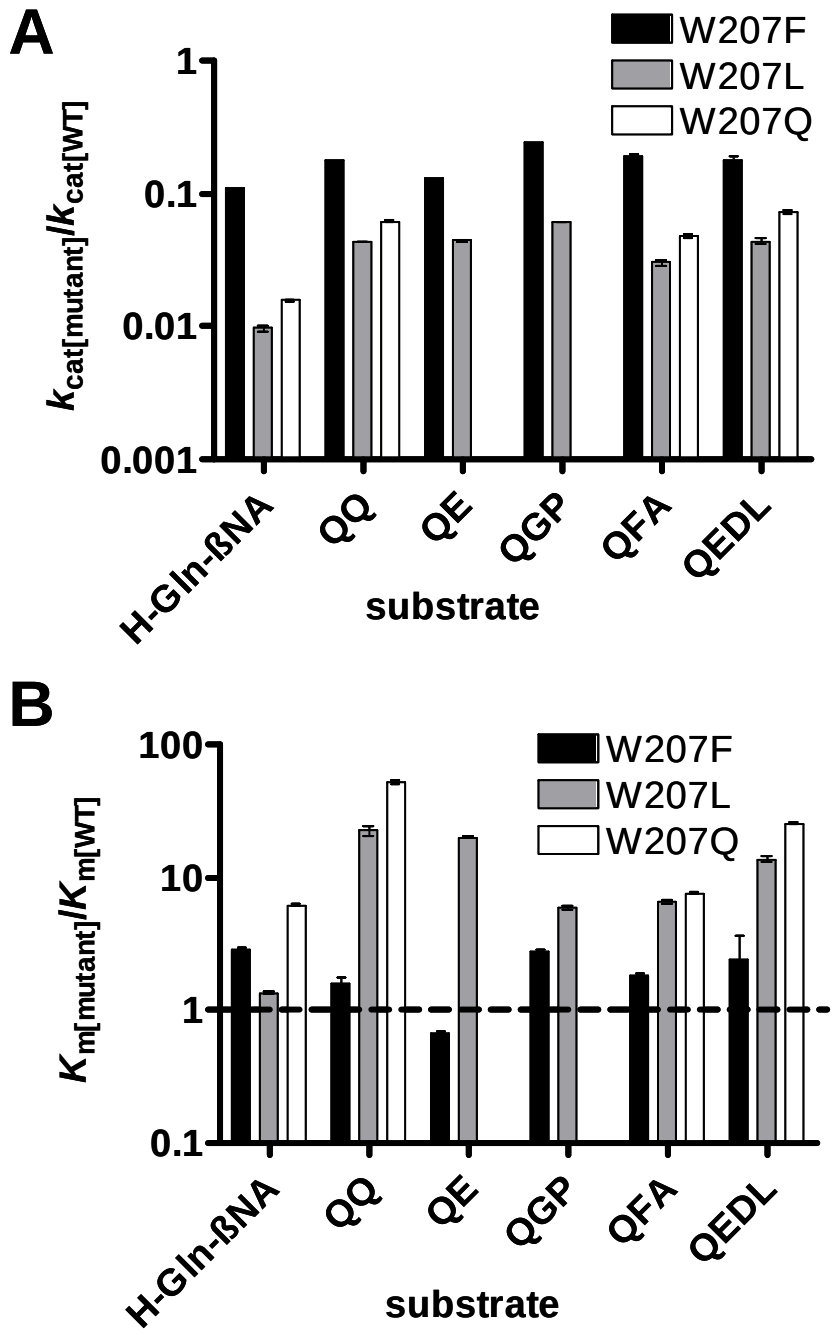

Figure S4: Catalytic parameters of the hQC variants $W^{207}F/L/Q$. **(A)** Ratio of the turnover number $k_{cat[mutant]}$ / $k_{cat[WT]}$ for hQC WT and W^{207} mutants. Replacement of W^{207} leads to a general reduction of k_{cat} to about 0.1 $k_{cat[WT]}$, independent of the introduced amino acid. The low activity of hQC $W^{207}Q$ did not allow a reliable determination of kinetic parameters k_{cat} and K_m with QE and QGP. **(B)** Ratio of the Michaelis-Menten constant $K_{m[mutant]}$ / $K_{m[WT]}$ for hQC WT and W^{207} mutants. While the mutation $W^{207}F$ has only a minor effect on K_m, introduction of less voluminous or polar amino acid residues leads to a pronounced increase of the value. Ratios ±SD were calculated based on discrete values of the corresponding hQC mutant and WT, each determined using three independent measurements. Reactions were carried out in 50 mM Tris, pH 8.0, at 30°C.

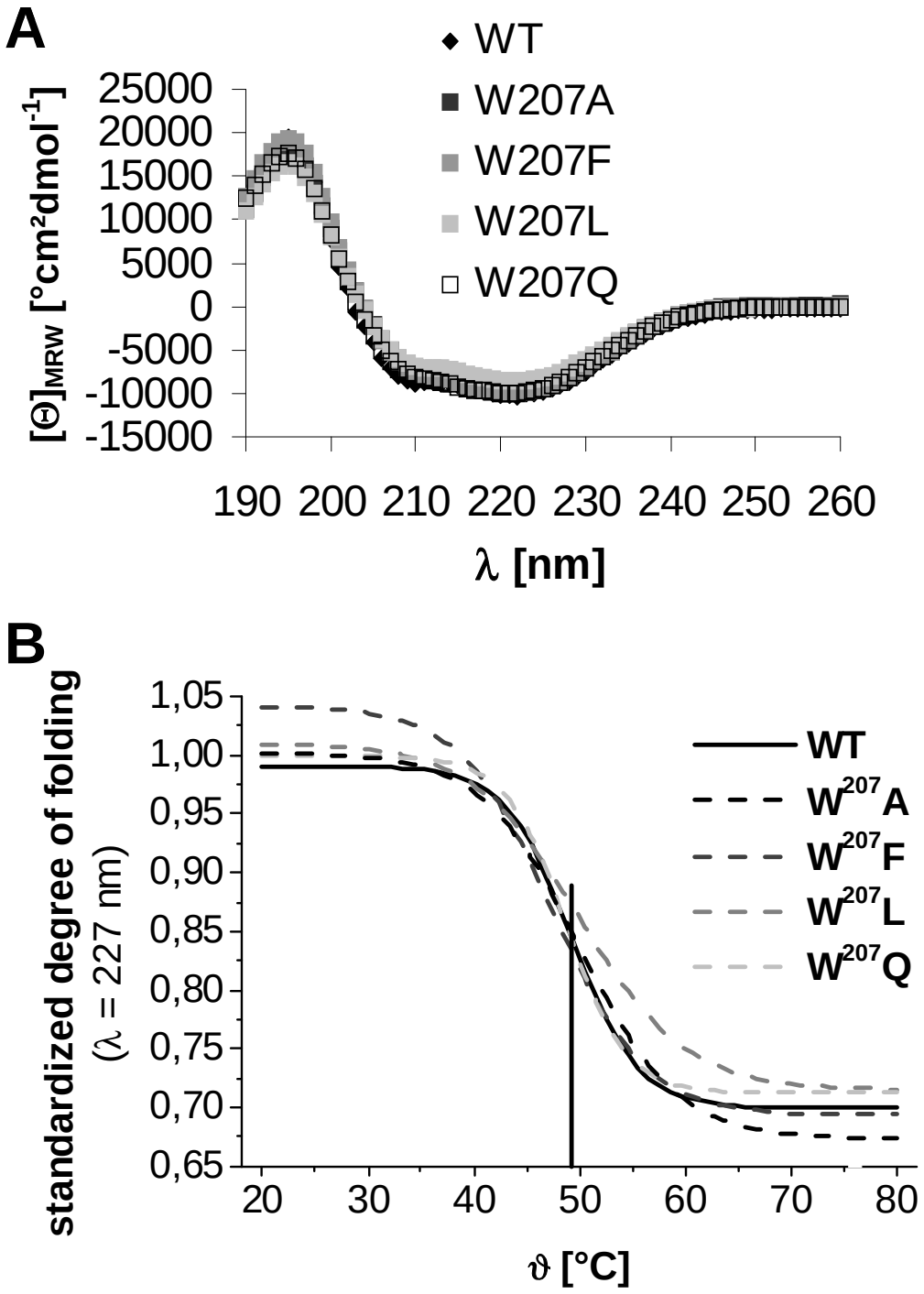

Figure S5: Far UV CD-spectra (190 nm < λ < 260 nm) of hQC WT and the W^{207} variants. **(A)** Comparison of the CD-spectra at 20°C (WT diamonds, variants squares). All enzymes show typical CD-spectra for proteins with a high α-helical content, characterized by minima of the mean residue ellipticity (θ_{MRW}) at 208 nm and 222 nm. **(B)** Sigmoidal fit of the temperature dependant change of the standardized mean residual ellipticity at 227 nm (continuous line WT, dashed lines variants). For all enzymes, $\vartheta_{1/2} \approx 49$°C was determined, indicating that W^{207} has no major influence on thermal stability. Proteins were dissolved in 10 mM potassium phosphate buffer, pH 6.8.

Table S5: Inhibitory constants for hQC WT

Inhibitor	K_i [μM]
Imidazole	147.7 ± 8.1
Benzimidazole	150.3 ±10.2
1-Methylimidazole	29.9 ± 3.8
1-Benzylimidazole	11.2 ± 0.7
N-ω-Acetylhistamine	24.0 ± 2.5
PQ50	0.10 ± 0.01
Cysteamine	31.0 ± 2.5

K_i values were determined in three independent evaluations with Gln-AMC as substrate in a concentration range between 4 and 0.25 K_m. Reactions were carried out in 50mM Tris, pH 8.0, at 30°C.

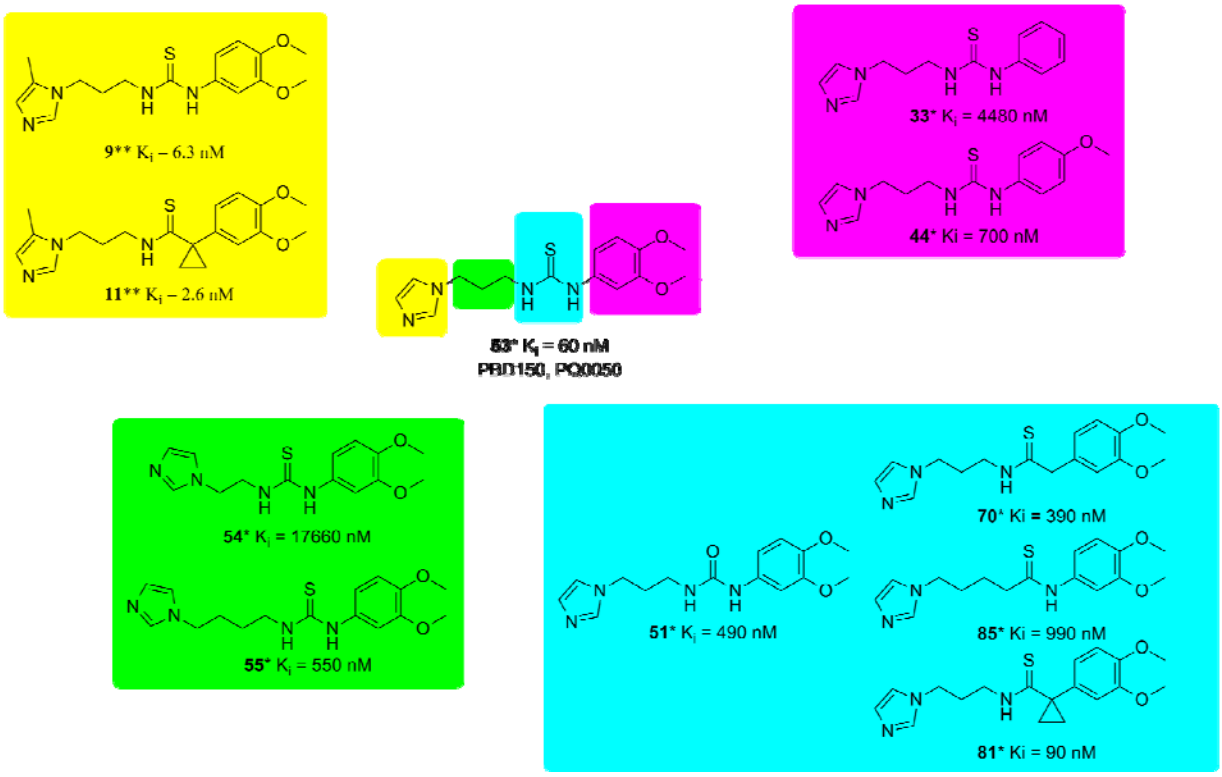

Figure S6: Structure activity relationships (SAR) for PQ50; data and compound numbers taken from *Buchholz *et al.* (2006) (ref. 28) and **Buchholz *et al.* (2009) (ref. 29).